

Turbulence suppression in combustion-driven magnetohydrodynamic channels

By J. C. REIS† AND C. H. KRUGER

Department of Mechanical Engineering, Stanford University, Stanford, CA 94305, USA

(Received 30 November 1983 and in revised form 4 August 1987)

The effects of a magnetic field on core turbulence, mean-velocity boundary-layer profiles, turbulence-intensity boundary-layer profiles and turbulent spectral-energy distributions have been experimentally determined for combustion-driven magnetohydrodynamic (MHD) flows. The turbulence suppression of the core was found to be similar to that of liquid-metal MHD flows, even though the turbulent structure was entirely different. The mean-velocity and turbulence-intensity boundary-layer profiles were affected much less than those of liquid-metal flows, primarily because the low-temperature thermal boundary layer reduced the electrical conductivity near the wall. No spectral dependence of turbulence suppression was observed in the core.

1. Introduction

Although the influence of a transverse magnetic field on the level and structure of turbulence in an electrically conducting fluid flow has been the subject of extensive research, virtually all of the published data have been obtained in liquid-metal flows. A second type of magnetohydrodynamic (MHD) channel flow is generated by the burning of fossil fuels with a seeding material added to enhance the electrical conductivity. Such flows, typically created by burning coal or natural gas with potassium as an ionizing seed, have some important differences from those of liquid-metal flows. Two of the most important differences are: (i) the structure of the free stream or core turbulence, and (ii) the varying conductivity through the thermal boundary layer.

Although the first detailed measurements of the influence of a magnetic field on liquid-metal flows were made a half century ago by Hartmann & Lazarus (1937), it was thirty years later when the first direct measurements of turbulence suppression were made by Branover, Slyusarev & Shcherbinin (1965). Additional measurements in rectangular ducts were subsequently made by Brouillette & Lykoudis (1967), Slyusarev (1969), Branover, Slyusarev & Shcherbinin (1970), Branover *et al.* (1970*a, b*), Slyusarev (1971), Hua & Lykoudis (1974) and Reed & Lykoudis (1978). Sukoriansky, Zilberman & Branover (1986) studied turbulent spectra and entrance effects.

Semi-empirical modelling of the influence of a magnetic field on turbulent boundary layers was begun by Harris (1960). Lykoudis & Brouillette (1967) developed a turbulence-damping model that modified the Prandtl formula for the

† Currently with Chevron Oil Field Research Co., La Habra, CA.

mixing length. One of the assumptions made in this model was that the turbulent eddy decays exponentially in time:

$$U = A \exp\left\{-\frac{\sigma B}{\rho}t\right\}. \quad (1)$$

Different choices for the characteristic time lead to somewhat different models. A similar theory was developed by Olin (1966). A somewhat different mixing-length model was developed by Branover (1968). A good survey of the experimental and theoretical work on liquid-metal MHD flow was given by Branover (1978). Lykoudis (1980) reported a successful agreement between a semi-empirical theory based on a damping model of the form given by (1) and experimental data for liquid-metal MHD flows.

The measurement of the effect of a magnetic field on combustion-driven MHD flows was first conducted by Olin (1966) using Pitot tube on the electrode wall, which is parallel to the magnetic field. He observed a trend toward a more laminar shape in the mean-velocity profiles. Sonju & Kruger (1969) made skin-friction measurements and observed a reduction in the skin friction at some Reynolds numbers with the application of a transverse magnetic field. Hartmann & Lazarus (1937) observed a similar effect and attributed the reduction in skin friction to turbulence damping.

The first direct measurements of turbulence damping in combustion-driven MHD flows were made by Rankin, Self & Eustis (1980) using a laser-Doppler velocimeter (LDV) on the insulator wall. With no electrical current applied, no observable effect of the magnetic field was seen on the mean-velocity profiles, although the turbulence level throughout the boundary level appeared to be reduced. Data were obtained for only one flow condition.

Barton (1980) and Kowalik (1980) made correlation measurements of fluctuating electrical parameters, and of the conductivity, respectively, and reported that the core turbulence was dominated by very long-lengthscale combustion streamers, and not wall-generated eddies.

2. Experimental facility

The present experiments were conducted in the Stanford M-2 combustion facility, shown schematically in figure 1. In this facility, ethanol was burned in pure oxygen with potassium added to enhance the conductivity. Nitrogen was added as a diluent for temperature control. The flow then went through a plenum chamber to allow the combustion process to come to completion, and to smooth out some of the combustion non-uniformities. The high-temperature plasma was then passed through a nozzle and into the main flow channel. After a run-in section of 0.56 m to allow the boundary layers to grow, the flow entered the active magnetic length of the channel. The measurements were made on the top electrode wall 0.10 m from the exit of the 0.61 m active magnetic length. The channel was 0.05 m wide by 0.076 m high. The flow then passed through a 0.30 m exit section and was sent to an exhaust clean-up system. The combustor, plenum and channel were water cooled and had an MgO brick lining to insulate the stainless-steel structure from the hot gas. The channel was operated at open-circuit electrical conditions, and the maximum magnetic field strength was 1.95 T. Because of the channel size, the boundary layers had begun to merge at the measurement location.

As the purpose of this research was to focus on the fluid-mechanical aspects of

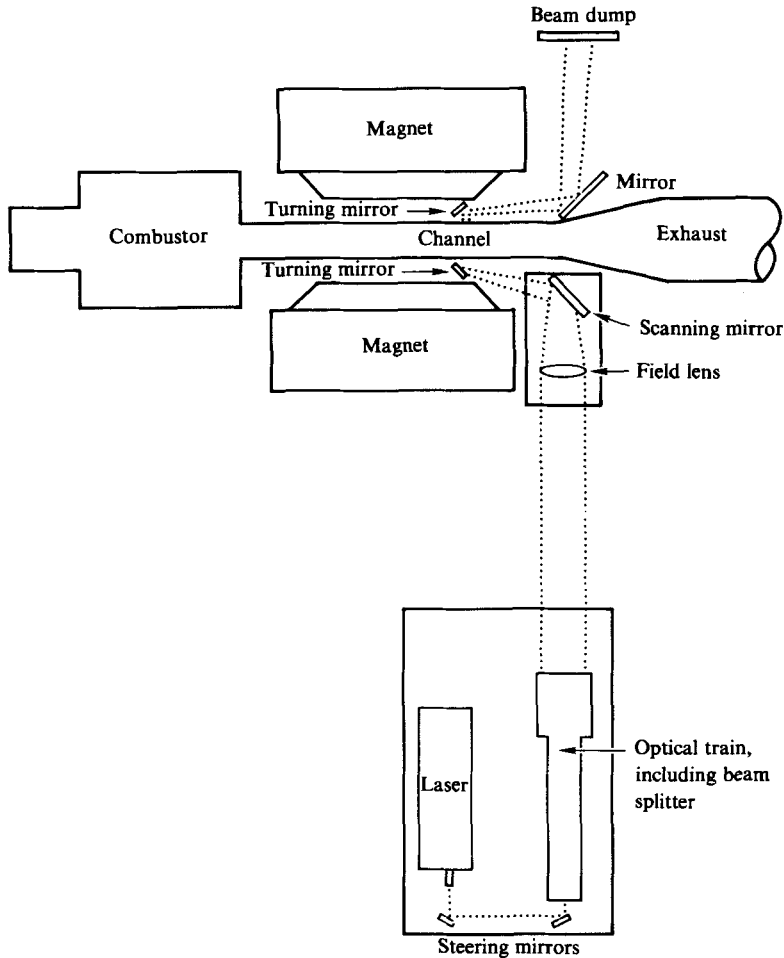


FIGURE 1. Schematic of LDV system with MHD flow train.

MHD, rather than on LDV system development, commercially available equipment was used wherever possible, with in-house modifications being made as necessary. The measurements were made with a single colour, argon ion, laser-Doppler-velocimetry (LDV) system operating in a backscatter mode (TSI-9100-6), with a burst counter (TSI-1990-A) and a digital computer interface (TSI-1998). This interface contains a timer that measures the time between validated particle measurements. The laser wavelength selected was 514.5 nm and the fringe spacing was 7.26 μm . The measured beam crossing half-angle was 2.03°.

The data acquisition system centred around an HP-21MX minicomputer. When a measurement was validated by the counter, it was sent to the computer along with the measured time from the last validated signal. When the computer core was filled, the data were written in its packed format onto magnetic tape, 3–16 bit words per particle measurement. The core could hold 9000 data points. A second program then read the data back into the computer for on-line analysis, if desired. Post-test data reduction included estimates for the power-spectral density function, obtained by using the time between validated measurements. The algorithm used was the discretized lag method for producing an autocorrelation function for random time-

sampled data, reported by Gaster & Roberts (1975). The power spectra were obtained by fast Fourier transforming the autocorrelation function, which was smoothed by a Hanning cosine window.

As with many LDV systems, it was necessary to artificially seed the flow with particles. The scattering centres selected were micron-sized zirconia particles, ZrO_2 . They proved capable of withstanding the thermal shock and high temperatures of passing from room temperature to an ethanol flame of 2800 K. To supply the particles to the flow, they were suspended in a slurry of alcohol and glycerine. This paste was loaded into a piston/cylinder and injected into the alcohol feed line. On a volume basis the proportions used were five parts zirconia, five parts alcohol and one part glycerine. These proportions were chosen so that the paste was too thick for the particles to settle out during the time of the experiments, but thin enough to be injected into the fuel and mix well.

Although the potassium provides the needed ionization to the flow, it also has some strong resonance emission lines in the spectral range of the photomultiplier sensitivity. A custom 1.0 nm wide laser line colour filter was designed and placed in the optical train to remove the unwanted radiation.

Because of the size of the magnet and the strength of its field, some severe restraints were placed upon the optical system to provide access to the plasma inside the active magnetic section of the channel. Because measurements were desired on the electrode walls, the laser beams had to pass through the plasma parallel to the field. This required compact non-magnetic optical components inside the powerful magnetic field. These were coupled to larger optical components outside the magnet with a long optical throw to cross the laser beams inside the plasma. The optical system is also shown schematically in figure 1. To provide optical access to the plasma, two open ports were cut into the channel. One problem with this configuration is the closeness of the two turning mirrors to the plasma. During normal operation, the pressure in the channel was slightly subatmospheric, but pressure transients could cause the hot flame to impinge directly on the mirrors. To minimize this problem, movable shutters were constructed to close the ports during changes in flow conditions, and the mirrors were replaceable in the event they were damaged. Entrainment through the ports was typically 0.1% by volume of the combustion flow.

The variance of the power-spectral density functions can be found from the analysis by Gaster & Roberts (1975),

$$\text{Var}[S'(\omega)] = \frac{3\lambda M \Delta\tau}{4N} \left[S(\omega) + \frac{C(0)}{\lambda} \right]^2, \quad (2)$$

with the standard deviation being the square root of the variance. Here, $S'(\omega)$ is the estimated spectrum, λ is the data rate, M is the total number of lag intervals computed, $\Delta\tau$ is the width of the lag interval, N is the total number of data points used, $S(\omega)$ is the true spectrum and $C(0)$ is the zero-lag value of the autocorrelation function, which is equal to the square of the turbulent velocity. Hence, it is seen that the uncertainty in the power-spectral density function is a function of the data rate, the total number of data points obtained and the magnetic-field strength. The dependence on the magnetic-field strength is through $C(0)$, which is reduced as the turbulence is damped. The data rate was on the order of 1000–2000 measurements per s. Srikantiah & Coleman (1985) conducted studies of turbulence-spectra measurements in combustion plasmas using LDV, but did not make turbulence-suppression measurements.

3. Experimental results

Turbulence suppression data were obtained in the core and in the electrode-wall boundary layer at Reynolds numbers from 1.3×10^4 to 2.1×10^4 and Hartmann numbers from 0 to 59. These values are based upon the channel hydraulic diameter, the bulk fluid velocity and the fluid properties in the relatively isothermal core. The measured electrical conductivity in the core varied from 5.1 to 21.6 mho/m, while the calculated density and viscosity varied from 0.109 to 0.130 kg/m³ and 7.61×10^{-5} to 8.55×10^{-5} Pa s, respectively.

Although the electrical conductivity was not measured in the boundary layer, its variation through the boundary layer can be estimated from temperature profiles measured by James & Kruger (1983). A typical core temperature of 2700 K and a wall temperature of 2200 K will yield an electrical conductivity at the wall 10 to 15 times lower than in the core.

The electrode wall was chosen for study because the Hartmann effect does not act upon the bulk flow on the electrode wall inside the magnetic field; hence this effect was somewhat separated from those of turbulence damping. Some alterations in the bulk flow on the electrode wall from axial magnetic-field gradients at the entry and exit of the active magnetic length do exist, however.

3.1. Turbulence suppression in the core

To compare the effect of a magnetic field on the turbulence dominated by combustion-driven streamers in the present experiments to the wall-generated turbulence in liquid-metal flows, the turbulence level in the core was measured with and without a magnetic field. Figure 2 shows the turbulence damping ratio, i.e. the turbulence level with magnetic field, as a function of the magnetic interaction parameter, $Ha^2/Re = \sigma B^2 L / \rho U$. The circles represent data obtained during the first day of testing, the squares from the second day of testing and the triangle from the data of Rankin *et al.* (1980).

If the data of Hua & Lykoudis (1974) are rereduced using the channel full width rather than the half-width, their data then indicate the same degree of turbulence damping as observed in the present study. Thus, there appears to be no significant difference between the effects of a magnetic field on the two types of flows, in spite of the large differences in the structure of the turbulence. The full width was chosen for the transverse turbulence lengthscale in the channel of Hua & Lykoudis because with their aspect ratio of 6 it is more analogous to the hydraulic diameter in the current study with an aspect ratio of 1.5. Following Lykoudis (1980), the data were also reduced as a function of $Ha^2/Re^{1.75}$. This form of the data is shown in figure 3. Note that these two scaling parameters, Ha^2/Re and $Ha^2/Re^{1.75}$, are the result of different assumptions for the characteristic time for the turbulence decay from (1).

In extending these data to full-scale MHD generators, it should be noted that the data appear to scale with the magnetic interaction parameter. In a large channel, however, the characteristic turbulence lengthscale should be, perhaps, the boundary-layer thickness rather than the channel hydraulic diameter. If a typical boundary-layer thickness is 10 cm, the flow velocity 800 m/s, magnetic-field strength 5.5 T, conductivity 6 mho/m and density 0.3 kg/m³, the turbulent magnetic interaction parameter would be 0.08. This is within the range measured in the Stanford facility, as shown in figure 2.

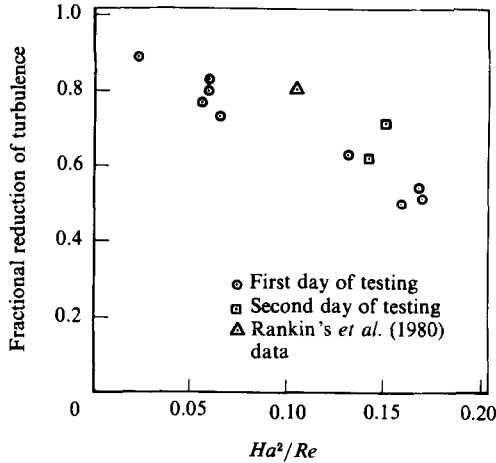


FIGURE 2. Damping ratio as a function of Ha^2/Re .

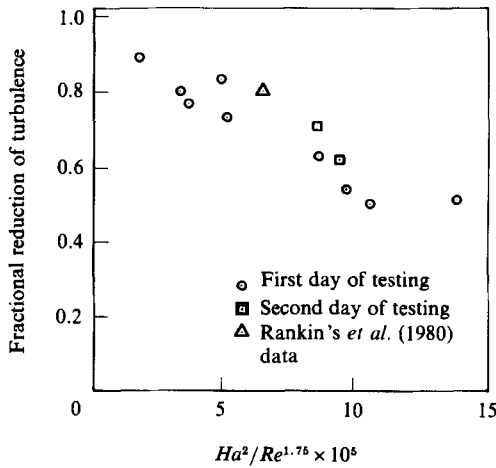


FIGURE 3. Damping ratio as a function of $Ha^2/Re^{1.75}$.

3.2. Mean-velocity boundary-layer profiles

To study the influence of a variable electrical conductivity, mean-velocity boundary layers were also measured at five flow conditions, with and without the magnetic field. Figure 4(a-c) shows three of these profiles for $Re = 1.38 \times 10^4$ and $Ha = 0, 30.4$; $Re = 1.74 \times 10^4$ and $Ha = 0, 48.0$; and $Re = 20.9 \times 10^4$ and $Ha = 0, 56.1$, respectively.

Although the change in the profiles with the application of a magnetic field is small, the power-law fit was consistently altered from a $\frac{1}{2}$ power law to a $\frac{1}{6}$ power law. Comparing this to the data of Branover *et al.* (1970) and Reed & Lykoudis (1978), and to the theory of Harris (1960) it is evident that the velocity profiles for the combustion-driven flows are not altered as strongly as those in the liquid-metal flows, even when the Hartmann effect is considered. Thus, even though the effect of the magnetic field upon the turbulence level in the core for combustion-driven flows is similar to that in liquid-metal flows, the effect on the mean-velocity profiles, and hence presumably skin-friction and heat-transfer coefficients, is smaller.

The mean-velocity profiles shown in figure 4(c) show a tendency towards the 'M-

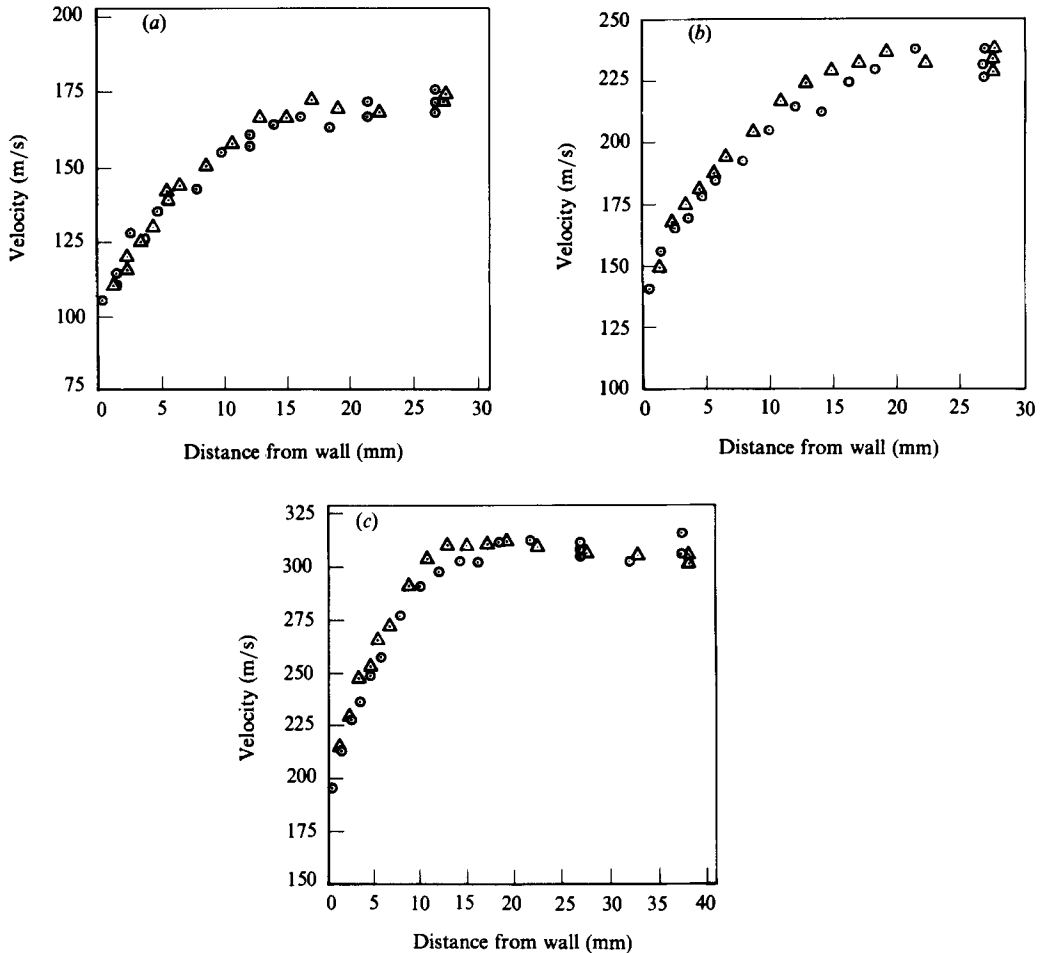


FIGURE 4. Electrode-wall mean-velocity boundary-layer profiles: (a) $Re = 13\,800$, $Ha = 0$ and 30.4 ; (b) $Re = 17\,400$, $Ha = 0$ and 48.0 ; (c) $Re = 20\,900$, $Ha = 0$ and 56.1 . \odot , $B = 0$; \triangle , $B = 1.95$ T.

shaped' profiles reported by Kit *et al.* (1970). Although the degree of overshoot for this flow condition is consistent with that reported by Kit *et al.*, no overshoot was observed for any other flow condition. In addition, the level of overshoot observed is lower than the uncertainty in the measurements. Therefore, there are probably insufficient data to determine whether the 'M-shaped' profile observed in figure 4(c) is a result of magnetic entry-length effects or experimental uncertainty.

3.3. Turbulence-intensity boundary-layer profiles

The reason for the weaker effect of the magnetic field on the mean-velocity profiles can be understood by examining the turbulence-intensity profiles shown in figure 5(a-c) which corresponds to the mean velocity profiles of figure 4(a-c) respectively.

Although the suppression of turbulence is observed in the core, little or no change in the turbulence level is observed in the boundary layer. This is believed to be the result of a much lower conductivity near the wall inhibiting the electrical currents from flowing between turbulent eddies. For liquid-metal flows, Hua & Lykoudis (1974) indicated a fairly uniform level of damping throughout the boundary layer,

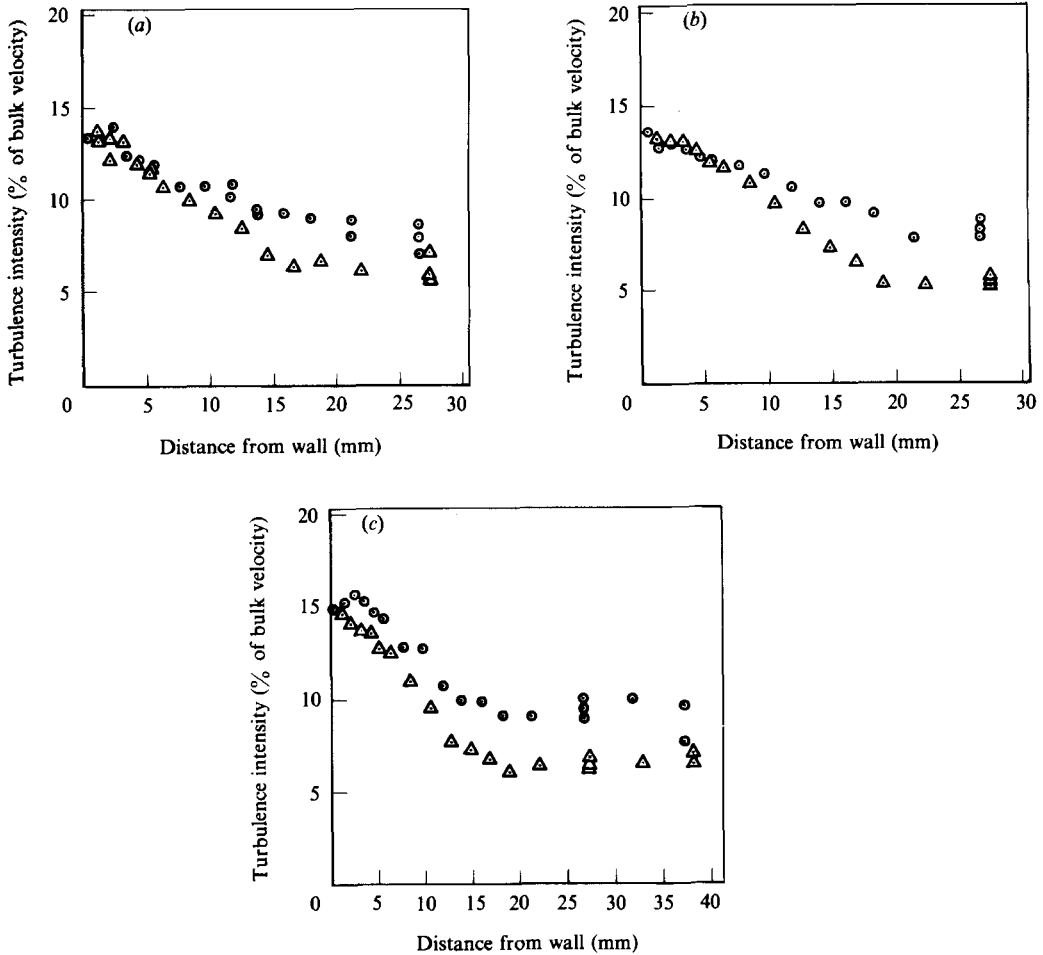


FIGURE 5. Electrode-wall turbulence-intensity boundary-layer profiles: (a) $Re = 13800$, $Ha = 0$ and 30.4 ; (b) $Re = 17400$, $Ha = 0$ and 48.0 ; (c) $Re = 20900$, $Ha = 0$ and 56.1 . \odot , $B = 0$; \triangle , $B = 1.95$ T.

while Reed & Lykoudis (1978) reported somewhat less of an effect near the wall. The suppression level observed by Reed & Lykoudis, however, was substantially more than that observed in the present study.

Since wall-generated turbulence is a result of instabilities near the wall, and since this cool region has a low electrical conductivity in combustion-driven flows, it is not surprising that the magnetic field affects the growth of the instabilities to a lesser degree than in the constant-conductivity liquid-metal flows. The high level of core turbulence present in the flow without a magnetic field was generated from combustion non-uniformities and streamers being convected past the measurement point.

3.4. Power-spectral density functions

To study the frequency response of turbulence to the magnetic field, autocorrelation and power-spectral density functions were obtained in the core, both with and without a magnetic field, for a variety of flow conditions and magnetic-field strengths.

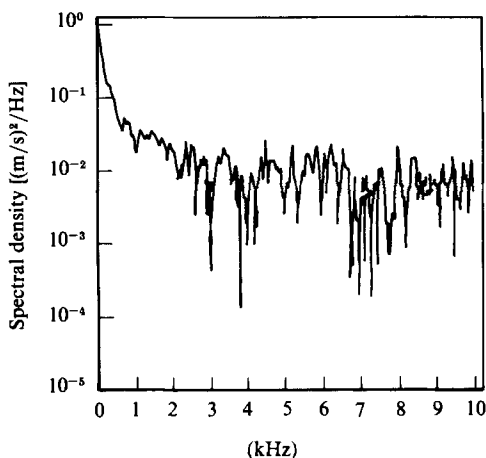


FIGURE 6. Typical power-spectral density function, without magnetic field.

From a study of the autocorrelation functions, it was seen that the velocity was correlated over roughly one ms, yielding correlation lengths on the order of tens of cm; much longer than that expected from wall-generated turbulence. This correlation is from the streamer structure and is consistent with the measurements of Kowalik (1980) and Barton (1980). It was also observed that the magnetic field did not alter the shape of the autocorrelation function or the correlation time, but only decreased the magnitude of the unnormalized correlation function. This is consistent with streamers forming upstream of the magnetic field and being convected through the active magnetic region, without the magnetic field affecting their formation. Hence, only the relative intensity of the streamers is affected, not the structure.

Power-spectral density functions were obtained by Fourier transforming the autocorrelations. These spectral density functions indicated that the bulk of the turbulent energy was contained at the low frequencies associated with combustion non-uniformities.

After computing the turbulent energy contained at various frequency intervals and comparing the cases without a magnetic field to the corresponding cases with a magnetic field, no trend in the variation of turbulence suppression with frequency was observed. The dominant, low-frequency structures were reduced to the same degree as higher-frequency structures. Nine sets of power spectra, both with and without a magnetic field, were analysed. Random variations in the frequency dependence caused by experimental and statistical uncertainties were observed for individual spectra, however.

Two typical spectral density functions are shown in figures 6 and 7 without and with the magnetic field, respectively. The flat spectra above a few kHz are not real. They are the result of the variance of the power spectra, and are in agreement with the theoretical variance predicted by (2).

3.5. Discussion of turbulence suppression

As shown by Barton (1980), Kowalik (1980) and the spectral data of this study, the predominant velocity fluctuations in the Stanford combustion-driven MHD facility were very long-lengthscale, low-frequency streamers. These streamers were generated in the plenum, stretched through the nozzle and convected through the magnetic field. They often had axial lengthscales longer than the active magnetic length of the

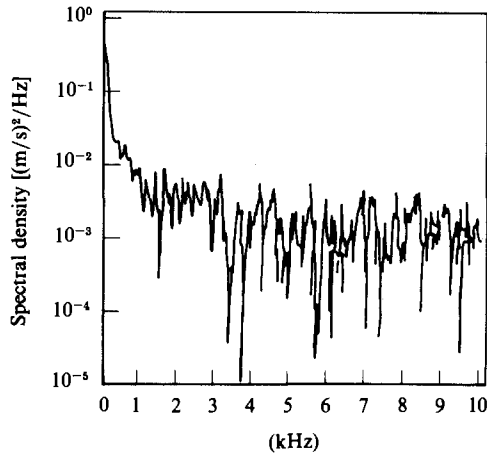


FIGURE 7. Power-spectral density function, with magnetic field, corresponding to figure 6.

channel. With this turbulence structure, the effects of the magnetic field on the turbulence from velocity gradients parallel to the direction flow (and perpendicular to the magnetic field) would be minimal. Even with this turbulence structure, the combustion-driven turbulence was suppressed to the same degree as conventional turbulence in liquid-metal flows, when the data were normalized by the transverse lengthscale, i.e. the lengthscale parallel to the magnetic field.

Gotoh (1960), and later Branover (1978), reported that two-dimensional turbulence will not be affected by a magnetic field if the axis of rotation is parallel to the magnetic field. Stated differently, without velocity gradients parallel to the magnetic field, there is no turbulence damping, regardless of the level of turbulence perpendicular to the magnetic field.

However, the semi-empirical models for turbulence suppression of the type proposed by Lykoudis & Brouillette (1967), Olin (1966) and Lykoudis (1980), assume that turbulence suppression operates on the velocity fluctuations perpendicular to the magnetic field. Nevertheless, these semi-empirical models provide satisfactory agreement with the liquid-metal data, as shown by Lykoudis (1980).

This apparent inconsistency is resolved if the local variations in the velocity gradient parallel to the magnetic field are the predominant factor in turbulence suppression in liquid-metal flows. The success of the semi-empirical models is because the turbulent lengthscales parallel and perpendicular to the magnetic field for liquid-metal flows are similar. The lengthscale enters into the semi-empirical models when determining the characteristic time in (1).

To model the suppression of the turbulent eddies in the cooler boundary layers of the combustion-generated magnetohydrodynamic flows, it is recommended that the semi-empirical models developed for liquid-metal MHD flows be used with the local fluid properties, e.g. electrical conductivity. Modelling the data obtained in this study was not possible, because of a lack of a computer program capable of modelling the non-MHD combustion streamers. The development of such a program was beyond the scope of this study.

REFERENCES

- BARTON, J. 1980 Fluctuations in combustion-driven MHD generators. Ph.D. thesis, Stanford University, Stanford, CA, USA.
- BRANOVER, H. 1968 *Magnitnaya Gidrodinamika* **3**, 3.
- BRANOVER, H. 1978 *Magnetohydrodynamic Flow in Ducts*. Wiley.
- BRANOVER, H., GEL'FGAT, YU., KIT, L. & PLATNIEKS, I. 1970a *Magnitnaya Gidrodinamika* **3**, 41.
- BRANOVER, H., GEL'FGAT, YU., KIT, L. & TSINOBER, A. 1970b *Mekh. Zhid. i Gaza* **2**, 35.
- BRANOVER, H., SLYUSAREV, N. & SHCHERBININ, E. 1965 *Magnitnaya Gidrodinamika* **1**, 1.
- BRANOVER, H., SLYUSAREV, N. & SHCHERBININ, E. 1970 *Magnitnaya Gidrodinamika* **4**, 54.
- BROUILLETTE, E. & LYKODIS, P. 1967 *Phys. Fluids* **5**, 995.
- GASTER, M. & ROBERTS, J. 1975 *J. Inst. Maths. Applics.* **15**, 195.
- GOTOH, K. 1960 *J. Phys. Soc. Japan* **4**, 696.
- HARRIS, L. 1960 *Hydromagnetic Channel Flows*. MIT Press and Wiley.
- HARTMANN, J. & LAZARUS, F. 1937 *Danske Videnskab. Selskab. Mat.-Fys. Medd.* **15**, 7.
- HUA, H. & LYKODIS, P. 1974 *Nucl. Sci. Engng* **54**, 445.
- JAMES, R. K. & KRUGER, C. H. 1983 *AIAA J.* **21**, 679.
- KIT, L., PETERSON, D., PLATNIEKS, I. & TSINOBER, A. 1970 *Magnitnaya Gidrodinamika* **4**, 47.
- KOWALIK, R. 1980 Measurements of conductivity nonuniformities and fluctuations in combustion MHD plasmas. Ph.D. thesis, Stanford University, Stanford, CA, USA.
- LYKODIS, P. 1980 *MHD Flows and Turbulence*, p. 27. Israel University Press.
- LYKODIS, P. & BROUILLETTE, E. 1967 *Phys. Fluids* **5**, 1002.
- OLIN, J. 1966 Turbulence suppression in magneto hydrodynamic flows. Ph.D. thesis, Stanford University, Stanford, CA, USA.
- RANKIN, R., SELF, S. & EUSTIS, R. 1980 *AIAA J.* **9**, 1094.
- REED, C. & LYKODIS, P. 1978 *J. Fluid Mech.* **84**, 147.
- SLYUSAREV, N. 1969 *Magnitnaya Gidrodinamika* **4**, 147.
- SLYUSAREV, N. 1971 *Magnitnaya Gidrodinamika* **1**, 18.
- SONJU, O. & KRUGER, C. 1969 *Phys. Fluids* **12**, 2548.
- SRIKANTIAH, D. & COLEMAN, H. 1985 *Exp. Fluids* **3**, 35.
- SUKORIANSKY, S., ZILBERMAN, I. & BRANOVER, H. 1986 *Exp. Fluids* **4**, 11.